JOURNAL OF MATERIALS SCIENCE 26 (1991) 3009–3018

Solid-state NMR elucidation of the role of mineralizers in the thermal stability and phase transformations of kaolinite

J. ROCHA, J. KLINOWSKI
Department of Chemistry, University of Cambridge, Lensfield Road, Cambridge CB2 1EW, UK
J. M. ADAMS
ECC International Limited, Pentewan Road, St Austell, Cornwall PL25 4DJ, UK

The effect of lithium nitrate mineralizer on the thermal stability and phase transformations of kaolinite has been studied using ^{7}Li, ^{27}Al and ^{29}Si magic angle spinning (MAS) nuclear magnetic resonance (NMR) in tandem with Fourier transform infrared spectroscopy (FTIR), X-ray diffraction (XRD) and TEM. As the temperature is raised, lithium nitrate melts, wets the surface of the kaolinite particles, and Li^{+} diffuses into the bulk of the crystals. The mineralizer retards the dehydroxylation of kaolinite by 15–20 °C. ^{27}Al MAS NMR indicates that metakaolinite originating from mineralized kaolinite contains less five-coordinated and slightly more four-coordinated Al. This promotes the transformation of metakaolinite into high-temperature phases which contain only four- and six-coordinated Al. Thus at 920 °C, mineralized samples (MS) contain γ-alumina type spinel but non-mineralized samples (NMS) do not. At higher temperatures, MS and NMS contain different amounts of spinel phase, mullite and cristobalite. ^{29}Si MAS NMR shows that cristobalite crystallizes from segregated amorphous silica. The process is reversed between 1300 and 1400 °C in MS (but not in NMS) and cristobalite vitrifies. This is probably caused by the lowering of the liquid temperature and subsequent rapid quenching of the melt.

1. Introduction

The physical and chemical properties of ceramic materials based on kaolin are related to the presence of crystalline and amorphous high-temperature phases. A number of compounds, known as mineralizers, have been used to promote or induce selectively the formation of certain species. For instance, small amounts of impurities such as alkali, alkaline-earth, iron and titanium oxides enhance the formation of mullite [1, 2]. However, the concept of a mineralizer is not restricted to the artificially introduced compounds. Most natural kaolinites contain chemical and mineralogical impurities in a wide range of concentrations, and it is likely that the differences in the behaviour and reactivity of kaolinites upon calcination are due to their presence. Thus, the study of mineralizers contributes to the understanding of the structure and reactivity of natural kaolinite and related high-temperature (meta) phases.

Only in a few cases are the mineralizing mechanisms reasonably well understood. The reasons for this are: (i) different mineralizers seem to have different effects, and in many cases more than one mechanism contributes to their action; (ii) several experimental techniques need to be deployed simultaneously; (iii) it is necessary to examine processes occurring throughout a very wide temperature range; (iv) metakaolinite is quasi-amorphous which poses difficulties before the conventional techniques of structural elucidation.

Solid-state nuclear magnetic resonance (NMR) has not previously been used to study the effects of mineralizers in clay systems. Because the technique probes local rather than long-range order, it does not suffer from the drawbacks inherent in other structural methods. Furthermore, the concentration of lithium cannot be monitored by the conventional solid-state analytical techniques such as X-ray fluorescence and analytical electron microscopy.

We have examined the mineralizing action of $LiNO_3 \cdot 3H_2O$. Preliminary work with other nitrates (see Section 2) showed that lithium nitrate is the most effective in promoting structural transformations. In particular, at 1100 °C samples mineralized with lithium nitrate contain the largest amount of mullite. Other effective mineralizers are the magnesium and calcium nitrates [3]. We show that solid-state NMR can be used in tandem with other techniques to monitor the action of mineralizers.

2. Experimental procedure

2.1. Samples

The highly crystalline (Hinckley index 1.24, [4]) Cornish kaolinite contained 3 wt % mica, 0.18 wt %

0022–2461/91 $03.00 + .12

TiO_2 and 0.40 wt % Fe_2O_3. About 80% of the particles were smaller than 2 μm. The cation-exchange capacity (measured upon saturation with ammonium acetate) was 4.0 meq/100 g and the specific surface area (N_2) $\simeq 10\ m^2\ g^{-1}$. To assess the differences between natural kaolinites, another sample of kaolinite was used containing low levels of Fe_2O_3 and TiO_2 (0.54 and 0.01 wt %, respectively), but 1 wt % quartz, 5 wt % mica and 6 wt % felspar. 10 mol % $LiNO_3 \cdot 3H_2O$ was introduced into kaolinite by dry mixing and ball-milling for 20 min. TEM reveals that the clay particles were not affected by this treatment. The samples, in bed depths of 6–7 mm, were calcined in air for 1 h and then quenched to room temperature. Some experiments in which samples were cooled down slowly where also carried out. In similar studies, we tested the effect of sodium, potassium, calcium, magnesium and barium nitrates.

2.2. X-ray diffraction (XRD)

Powder XRD patterns were acquired using a Philips automatic diffractometer fitted with a vertical goniometer and CuK_α radiation selected by a graphite monochromator in the diffracted beam. *In situ* variable temperature studies used an Anton-Parr high-temperature attachment.

2.3. Fourier transform infrared spectroscopy (FTIR)

Spectra in the region 4000–400 cm^{-1} were recorded using a Nicolet MX-1 Fourier Transform spectrometer and the conventional KBr wafer technique. The wafers were outgassed at 160 °C for 1 h prior to obtaining spectra. The spectra were typically an average of 128 scans with 1 cm^{-1} resolution.

2.4. Magic angle spinning (MAS) NMR

^{29}Si MAS NMR spectra were measured at 79.5 MHz with a Bruker MSL-400 multinuclear spectrometer. An Andrew-Beams probehead was used with rotors spinning at 2.5–3 kHz with air as the driving gas. Radio-frequency pulses equivalent to 40° pulse angle were applied with a 30 s recycle delay. ^{29}Si chemical shifts are quoted (p.p.m.) from external tetramethylsilane (TMS). ^{27}Al MAS NMR spectra were measured at 104.2 MHz with very short and powerful (0.6 μs, equivalent to 9° pulse angle) r.f. pulses and a 0.2 s recycle delay. Rotors were spun in air at 4–5 kHz. Chemical shifts are quoted in p.p.m. from external $Al(H_2O)_6^{3+}$. ^7Li spin-lattice relaxation times were measured at room temperature using a saturation recovery pulse sequence. In all cases, the decay of the signal was very nearly a single-parameter exponential. The measurements were repeated three times for each sample.

2.5. Transmission electron microscopy

TEM was performed with Hitachi H-7000 and Jeol JEM 200 CX electron microscopes at 75 and 200 kV, respectively.

3. Results

3.1. XRD

The XRD patterns of mineralized (MS) and non-mineralized (NMS) samples of the highly crystalline Cornish kaolinite calcined at various temperatures are compared in Fig. 1, while the normalized intensities of the 0 0 1 reflections are given in Fig. 2. As dehydration proceeds, there is a linear decrease in the intensity of the 0 0 1 reflection, but it is clear that the long-range order of the mineralized kaolinite collapses at a temperature 15–20 °C higher than that of NMS. Between dehydration and 900 °C, XRD patterns are independent of the presence of the mineralizer. However, by 920 °C only the (quenched) MS give γ-alumina type spinel (see Srikrishna *et al.* [5] and references therein) reflections at 0.198 nm (Fig. 1c and d) and 0.140 nm; above that temperature all samples contained the spinel phase and mullite. Another sample of the parent kaolinite, relatively rich in mineralogical impurities (quartz, mica and felspar), mineralized with lithium nitrate and calcined at 920 °C, exhibited not only spinel reflections but also traces of mullite.

The XRD pattern of mineralized samples shows that a relatively large amount of mullite is already

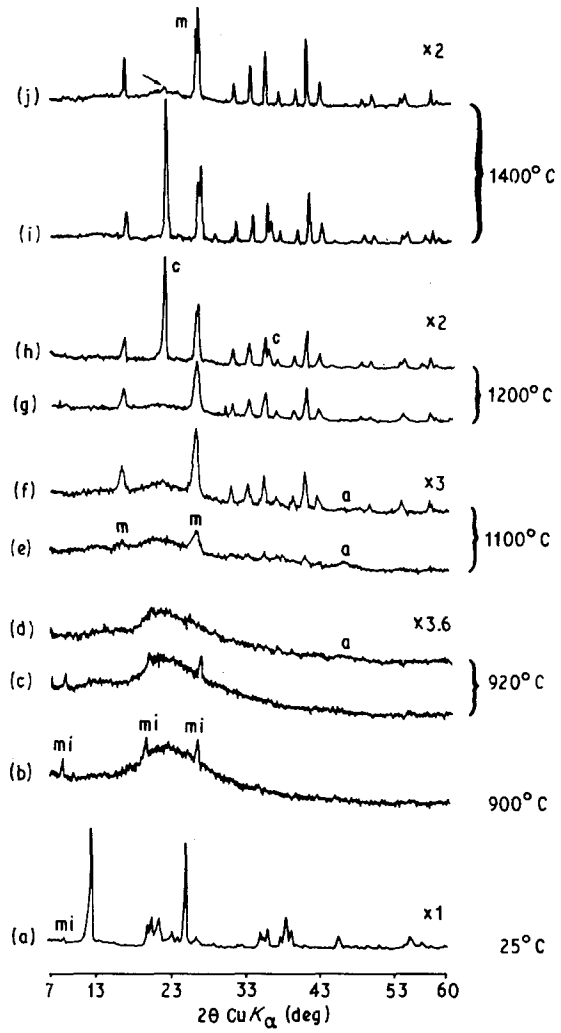

Figure 1 XRD patterns of non-mineralized (lower traces) and mineralized (upper traces) samples after calcination in air for 1 h at different temperatures. (a) and (b) are characteristic of kaolinite and metakaolinite, respectively, and are produced by both mineralized and non-mineralized samples. Impurities and phases: mi, mica; a, γ-alumina type spinel; m, mullite; c, cristobalite.

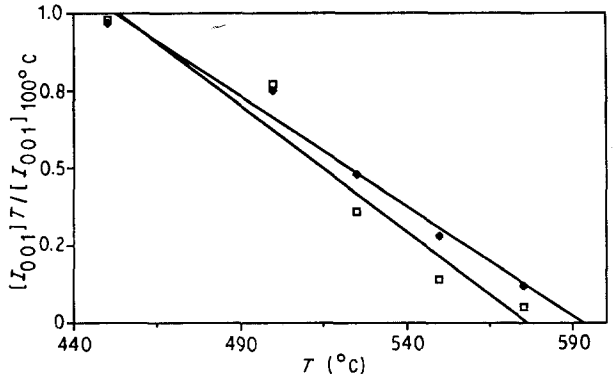

Figure 2 Variation of the intensity of the kaolinite 001 (*in situ*) XRD reflection normalized to the intensity of the 001 reflection (given by a sample calcined at 100 °C) plotted as a function of the temperature. (□) Non-mineralized samples, (◆) mineralized samples.

present at 1100 °C, along with traces of γ-alumina type spinel (Fig. 1f). By contrast, NMS are much poorer in mullite and richer in spinel phase (Fig. 1e). By 1200 °C all samples contain mullite but MS also contain cristobalite: in both cases, no spinel reflections are seen (Fig. 1g and h). At 1300 °C (not shown) all samples give well-developed reflections from cristobalite and mullite. Strong mullite reflections are observed in the XRD patterns of all samples calcined at 1400 °C, but only traces of cristobalite are found in MS samples. By contrast, NMS exhibit strong cristobalite reflections at 1400 °C which, although weaker, persist to 1500 °C along with those of mullite. At no temperature is there evidence for the presence of lithium silicates or aluminosilicates.

3.2. FTIR

The FTIR spectra of samples heated at 550 °C are given in Fig. 3. In the lattice vibration region, NMS (Fig. 3b) display a typical metakaolinite pattern (see Fig. 4a and for details see Rocha and Klinowski [6]). In the OH stretching region (Fig. 3b) only very faint kaolinite bands are observed. MS display relatively strong kaolinite OH stretching bands and a faint unresolved band at ~ 940 cm^{-1} assigned to Al–O–H bending modes (Fig. 3c). Between 600 and 900 °C there is no significant difference in the spectra of MS and NMS; a typical spectrum in given in Fig. 4a. By 920 °C, NMS display a more developed band at 665 cm^{-1} than do MS (Fig. 4b and c); the band is assigned [7] to Si–O stretching. We shall see later that, by contrast to NMS, only a very small amount of five-coordinated Al is present in MS. It is, therefore, possible that the metakaolinite band centred at ~ 665 cm^{-1} is also associated with five-coordinated Al. In the range 920–1400 °C, the FTIR spectra (Fig. 4d–g) of both MS and NMS are consistent with the presence of mullite, γ-alumina type spinel and cristobalite (for details see, for example, [7]) and fully support the XRD results.

3.3. MAS NMR

The ^{29}Si MAS NMR spectra of uncalcined MS and NMS (Fig. 5a) are identical and consist of a single

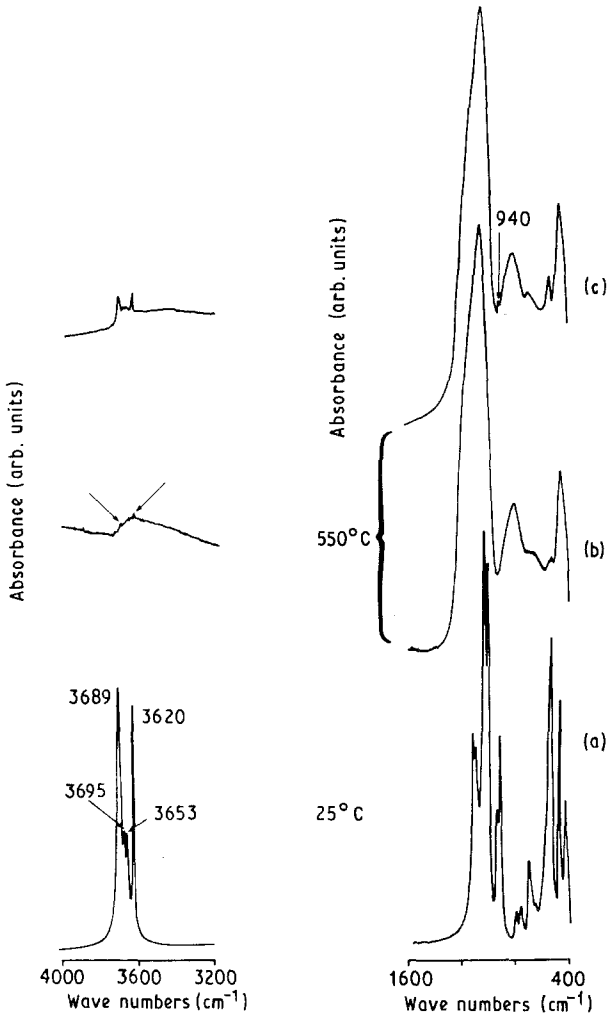

Figure 3 FTIR spectra (a) characteristic of both non-mineralized and mineralized kaolinite and (b, c) of non-mineralized and mineralized samples, respectively, calcined in air at 550 °C for 1 h. The vertical scale of the OH-stretching region (4000–3200 °C) is ~ 1.4 times more sensitive than that of the lattice-vibration region (1600–400 °C).

resonance at − 91.5 p.p.m. with full width at half maximum (FWHM) of 2.0 p.p.m., characteristic of layered silicates and assigned to the Q^3 environment (Si linked, via oxygens, to three other Si atoms). By 500 °C the spectrum from NMS (Fig. 5b) shows that the silicon matrix has undergone an important transformation and that a significant amount of metakaolinite has been formed [6, 8, 9]. In MS (Fig. 5c), the local silicon order is still similar to that found in kaolinite, and only a relatively small amount of metakaolinite is formed. Above 600 °C the spectra of all samples (Fig. 5d) are similar [6, 8]. At 920 °C (not shown) NMS display a resonance at approximately − 109 p.p.m. with a FWHM = 14.7 p.p.m. MS give a similar spectrum but the signal is centred at approximately − 108 p.p.m. and FWHM = 16.5 p.p.m. At 950–1000 °C the spectra of MS and NMS are very similar (Fig. 5e) and consist of one broad resonance (FWHM ~ 13.5 p.p.m.) centred at − 109 to − 110 p.p.m. from amorphous silica and perhaps cristobalite germs which are too small to be detected by XRD [6] and a shoulder at approximately − 87 p.p.m. from mullite. By 1100 °C (Fig. 6a and b) MS are clearly richer in mullite, as shown by the

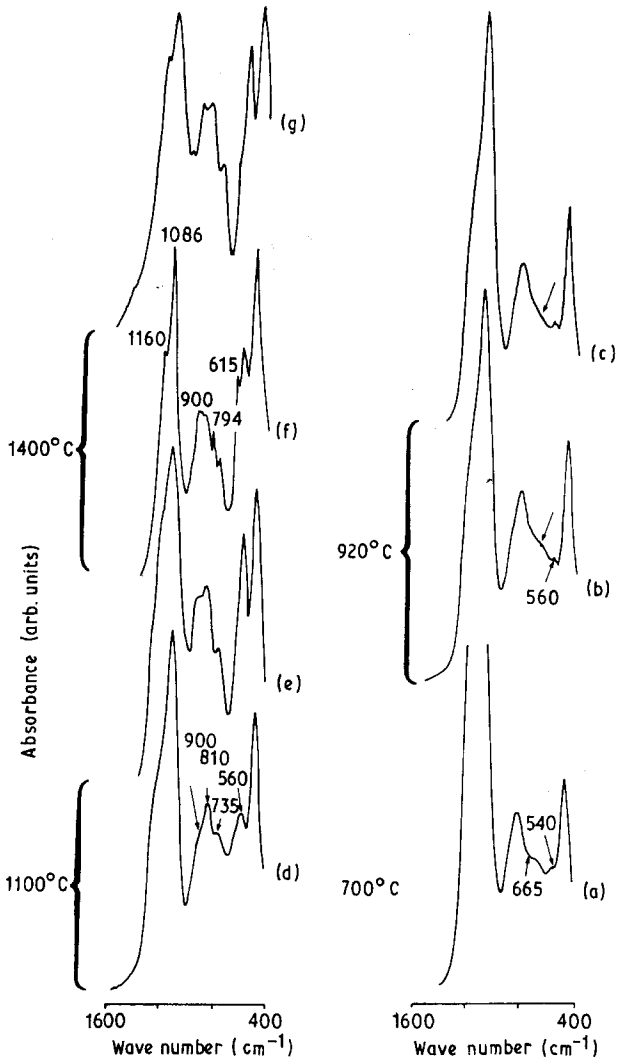

Figure 4 FTIR spectra of non-mineralized (b, d, f) and mineralized (c, e, g) samples calcined in air for 1 h at temperatures in the range 920–1400 °C. Notice the presence of sharp cristobalite bands at 615 and 794 cm^{-1} given by the NMS at 1400 °C which are absent from the spectrum of MS. For comparison, (a) shows a typical metakaolinite spectrum given by both mineralized and non-mineralized samples.

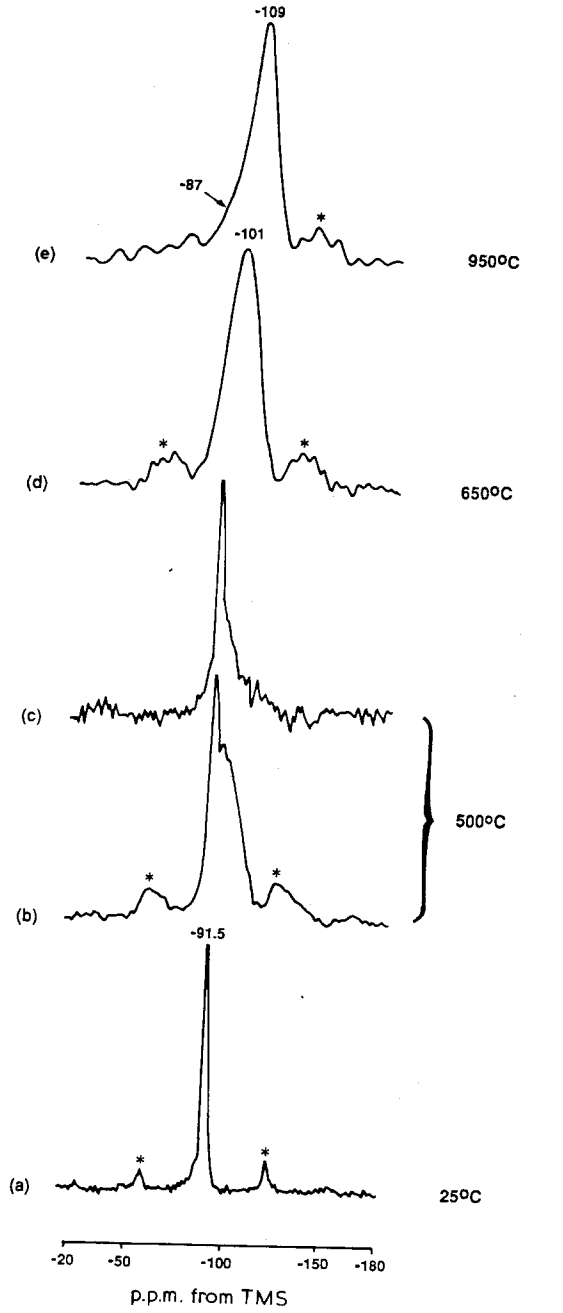

Figure 5 ^{29}Si MAS NMR spectra of (b, c) non-mineralized and mineralized samples, respectively. The spectra shown in (a, d and e) are characteristic of both non-mineralized and mineralized samples. (*) Spinning sidebands.

presence of a much stronger signal at − 87 p.p.m. Interestingly, the FWHM of the signal centred at − 110 p.p.m. is similar in all samples, which indicates that the amorphous silica pools of MS and NMS retain a similar degree of disorder. As shown in Fig. 6c, in MS calcined at ~ 1200 °C the amorphous silica begins to crystallize as cristobalite, although this is not observed in the NMS where only mullite continues to crystallize. At 1300 °C, all samples (Fig. 6d) contain cristobalite, mullite and some amorphous silica. At 1400 °C, MS give a broad resonance at − 110 p.p.m. (Fig. 6f) instead of the sharp cristobalite signal. No such broadening of the mullite resonance at − 87 p.p.m. is observed. On the other hand, in NMS (Fig. 6d and e) mullite and cristobalite continue to crystallize above 1300 °C; the FWHM of the cristobalite resonance at approximately − 112 p.p.m. decreases from 4.2–2.6 p.p.m. but even at 1400 °C a small amount of amorphous silica is still present.

The ^{27}Al MAS NMR spectra of all uncalcined samples are identical (Fig. 7a) with a single peak at ~ 0 p.p.m. (FWHM = 12 p.p.m.) assigned to six-coordinated Al. Above ~ 500 °C all samples exhibit two additional resonances (Figs 7b–i and 8a–d): at ~ 28 p.p.m., assigned to five-coordinated Al, and at ~ 57 p.p.m. due to four-coordinated Al (for details see [6, 8] and references therein). Examination of the spectra reveals that, at any given temperature, MS always contain less five-coordinated Al than NMS. Spectral deconvolution [6] suggests that in MS some of the aluminium which in NMS is five-coordinated is actually in four-fold coordination. However, in view of the uncertainties inherent to the line simulation procedure, this is not certain. At 920 °C the spectra from MS and NMS (Fig. 8c and d) differ substantially, particularly in the content of five-coordinated Al, but above 950 °C all samples give similar spectra. New species involving four- and six-coordinated Al are clearly in evidence: the ^{27}Al resonances are now at

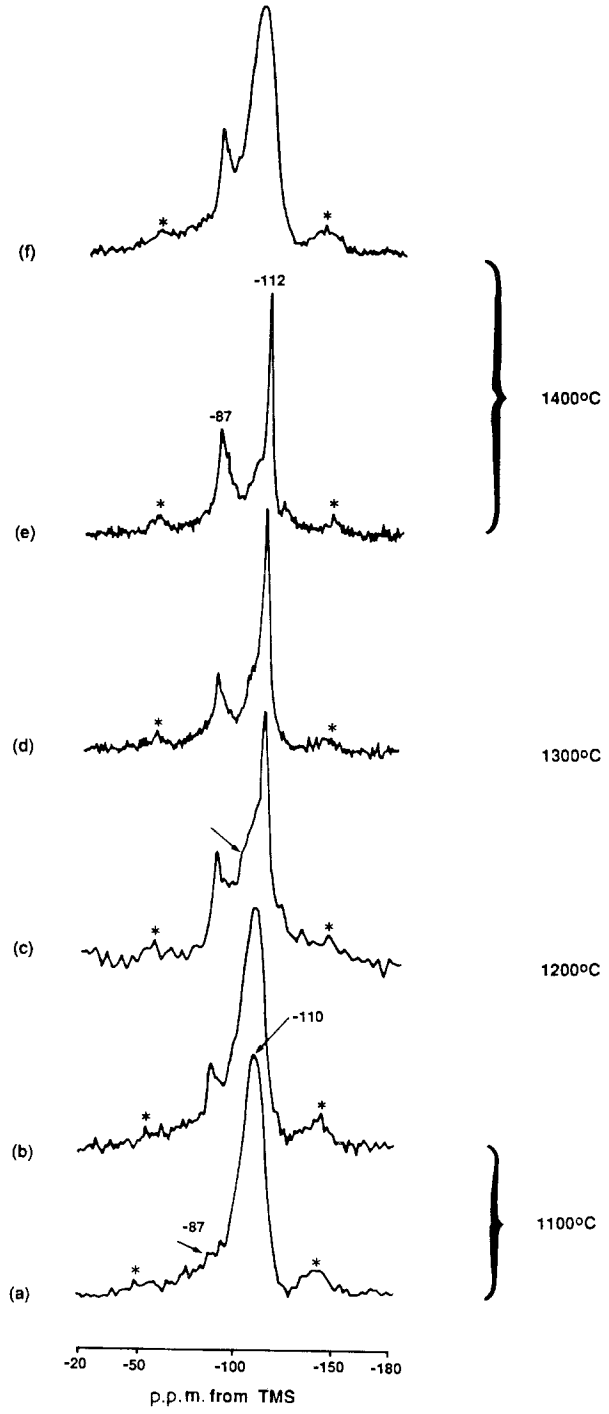

Figure 6 ^{29}Si MAS NMR spectra of (a, d, e) non-mineralized and (b, c, f) mineralized samples calcined in air for 1 h at temperatures in the range 1100–1400 °C.

63–66 p.p.m. and 2–4 p.p.m., respectively, while the FWHM increase considerably [6]. Sanz *et al.* [10] reported resonances at 0, 42 and 60 p.p.m. in 3:2 mullite. Pure γ-alumina resonates at ~ 7 and 70 p.p.m. (Fig. 9f). Thus, in the range 950–1100 °C the ^{27}Al spectra of all samples indicate the presence of both mullite and γ-alumina type spinel. At 1100 °C there are small but important differences between the spectra of NMS and MS (Fig. 9a and b). MS gives resonances (at − 1 and 53–55 p.p.m.) shifted to more negative values in comparison with those given by NMS (at 3–4 and 63–65 p.p.m.). Note also that above 1100 °C both kinds of sample produce spectra similar to those displayed by the 1100 °C MS (Fig. 9c and d). These observations suggest that above ~ 1100 °C the spinel phase is converted into mullite. By changing the spinning frequency of the MAS rotor and thereby removing the spinning sidebands from the spectral region of interest, we were able to show, in agreement with Sanz *et al.* [10], that above 1100 °C the three mullite resonances, at approximately − 1, 44 and 58 p.p.m., are present in all our samples (Fig. 9d and e).

The ^{7}Li MAS NMR spectra of uncalcined and calcined MS are shown in Fig. 10a and b, respectively. Only a small shift from − 1.2 to − 1.8 p.p.m. and an equally small increase in FWHM from 1.1–1.6 p.p.m. take place upon calcination at 600 °C. Treatment at other temperatures produces similar spectra, which contain little information of chemical interest. Quadrupole nutation NMR experiments [11] confirm that the small quadrupole moment of ^{7}Li does not favour the use of the technique to distinguish between quadrupolar species in different chemical environments. We have therefore resorted to the measurement of ^{7}Li T_1 spin-lattice relaxation times, and found them to vary considerably with the temperature of calcination (see Fig. 11). At room temperature, T_1 is short (~ 45 ms) probably due to the presence in the structure of lithium hydrate of water molecules which provide an efficient mechanism for relaxation. However, in samples calcined at higher temperatures, T_1 changes significantly (Fig. 11) whenever an important structural event occurs.

3.4. TEM

Fig. 12a and b show typical transmission electron micrographs of metakaolinite samples originating from MS and NMS kaolinite. No significant difference is found between the two groups. In MS calcined at 920 °C, very small (< 3–4 nm) spinel crystallites emerge from the amorphous matrix (Fig. 12c) and grow with increasing temperature. By 1100 °C, they are also clearly seen in NMS, particularly near the edges of the plates (Fig. 12d). At 1200 °C, mullite is the only crystalline phase present in NMS (Fig. 12e).

4. Discussion

Several techniques have confirmed that the mineralizer modifies the temperature at which particular phases are formed, and sometimes results in the production of a quite different phase. We shall consider the various aspects of the action of the mineralizer in turn.

4.1. Diffusion of Li^+

Above 450 °C, ^{7}Li T_1 values increase markedly. Göbel *et al.* [12] showed that relaxation of ^{7}Li at room temperature is dominated by the coupling of the lattice to the quadrupole moment of the nucleus which, because of ionic diffusion, is time-dependent. Thus the increase of ^{7}Li T_1 values is caused by a significant change in the ionic mobility of Li, occurring simultaneously with dehydroxylation. It is likely that diffusion of lithium cations is not restricted to the surface of the particles. If so, nucleation of high-temperature phases may not occur only on the crystal surface as maintained by some workers [13, 14]. This conclusion is supported by Gomes [15] who showed

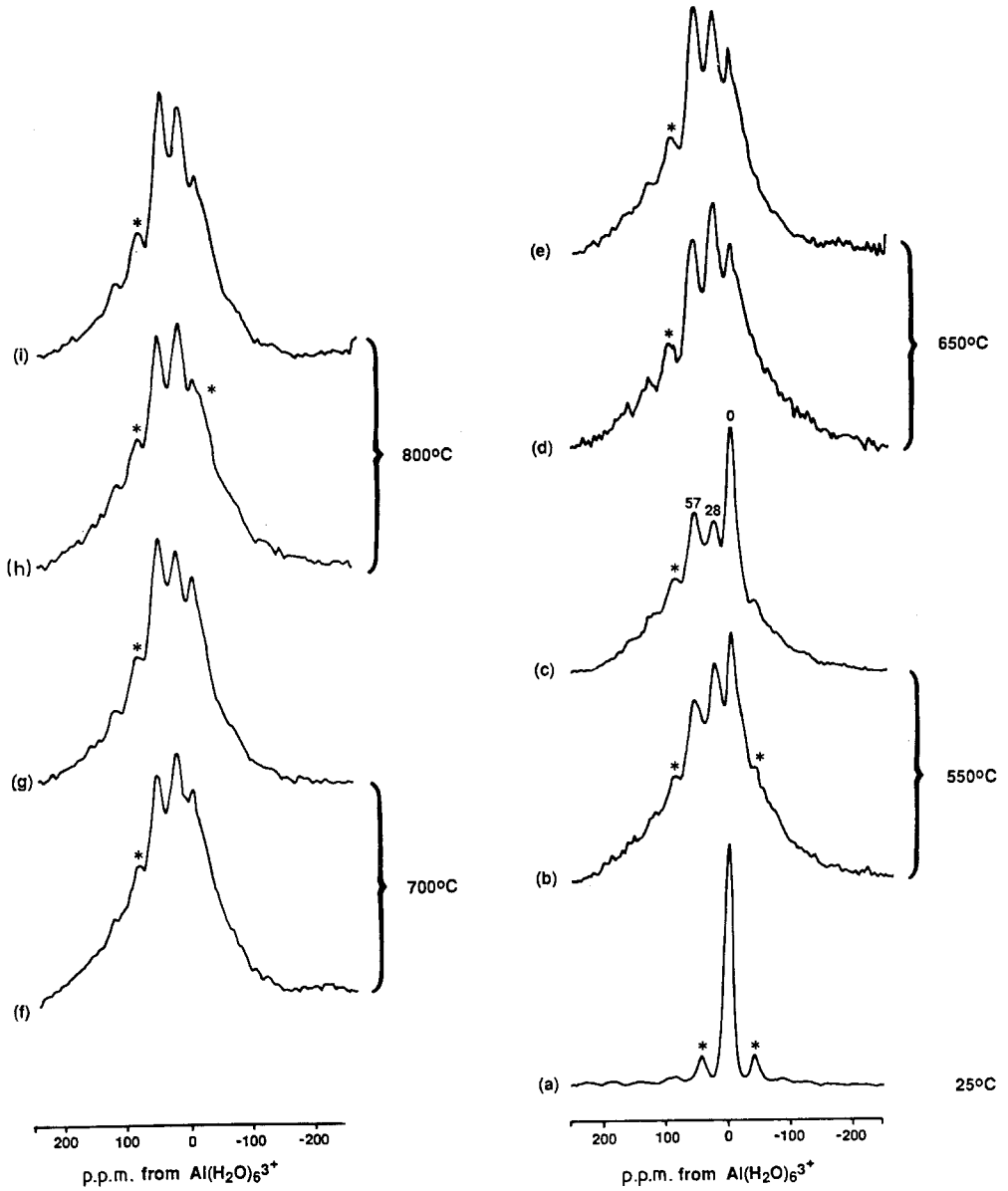

Figure 7 ^{27}Al MAS NMR spectra of (a) both non-mineralized and mineralized kaolinite, (b, d, f, h) non-mineralized and (c, e, g, i) mineralized samples calcined in air for 1 h at 550–800 °C. (*) Spinning sidebands.

that the mineralizing action is enhanced when the mineralizer is added to kaolinite: DMSO or kaolinite: hydrazine hydrate intercalates in which the mineralizer enters the intracrystalline space of kaolinite. Lemaitre and Delmon [3] showed that cationic diffusion must play an important role in the mineralizing mechanism. They investigated the shrinkage of kaolinite by isothermal dilatometry and found a correlation between the "initial shrinkage rates" at 900 °C (low-temperature isothermal shrinkage, LTS) produced by various mineralizers and their corresponding cationic radii. Many other studies confirm the importance of cationic diffusion in the mineralizing action of lithium salts [16, 17].

4.2. Action on the Al matrix of metakaolinite: inhibition of the formation of five-coordinated Al

The addition of lithium nitrate stabilizes the structure of kaolinite by an additional 15–20 °C. It has been suggested ([18] and references therein) that the dehydroxylation of kaolinite proceeds inwards from the edges of the grains parallel to the (0 0 1) planes. At first, OH groups may escape from the edges of the plates without diffusion throughout the grain, but later diffusion of H_2O from the interlayer region must occur. It is possible that the presence of the mineralizer stabilizes the kaolinite structure by impeding the diffusion of water, generating an intergrain vapour pressure and increasing the activation energy of dehydroxylation. Having stabilized the structure by 15–20 °C, lithium nitrate inhibits the formation of five-coordinated Al. We note that this capacity of a lithium salt to induce changes in coordination of other ions is not unique to the nitrate. For example, it has been reported [19] that addition of Li_2O to a GeO_2 glass transforms some tetrahedral germanium atoms to the octahedral coordination. Similarly, it is possible (but not certain, due to uncertainties inherent in spectral simulation) that in metakaolinite the mineralizer transforms some aluminium from five- to four-fold coordination.

4.3. Formation of γ-alumina type spinel and mullite

We suggest that γ-alumina type spinel and mullite appear in MS at lower temperatures than in NMS

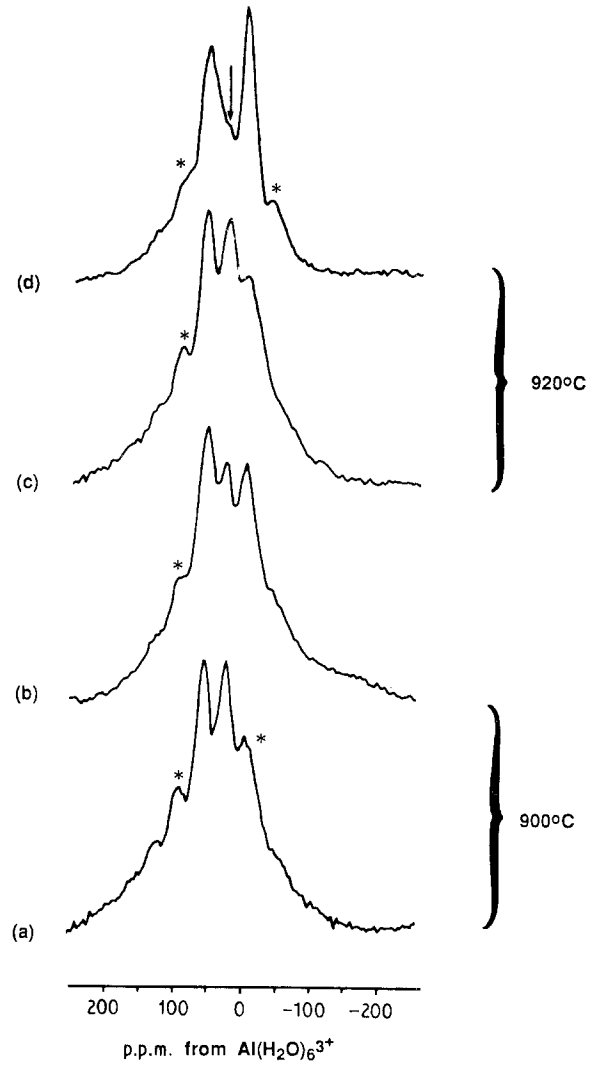

Figure 8 ^{27}Al MAS NMR spectra of (a, c) non-mineralized and (b, d) mineralized samples calcined in air for 1 h at 900 and 920 °C. (*) Spinning sidebands.

because both of these phases contain aluminium in four- and six-fold coordination: reactions starting from metakaolinite normally require transformation of five- into four- and six-coordinated Al. In this case, stability to conversion might well be lower if less five-coordinated Al is present. Note that at 920 °C the ^{29}Si spectrum of MS is similar to the 900 °C spectra of both MS and NMS. However, the resonance in the 920 °C spectrum of NMS is narrower than that given by those samples and in addition is also shifted towards − 110 p.p.m. Thus the mineralizer not only promotes the formation of spinel phase but also delays the transformation of the silica matrix which remains more disordered. Nevertheless, by 950 °C the ^{29}Si spectra of all samples are very similar. It is interesting to compare these observations with the work of Bulens *et al.* [14] on the mineralizing action of MgO and CaO. The LTS parameters of MgO at 900 °C are similar to those given by lithium nitrate and the authors speculate that the salt selectively segregates amorphous alumina and silica thus initiating further nucleation of γ-alumina. Our work shows that lithium nitrate promotes the formation of spinel phase, but instead of inducing segregation of more amorphous silica it simply delays the ordering of the silica pool.

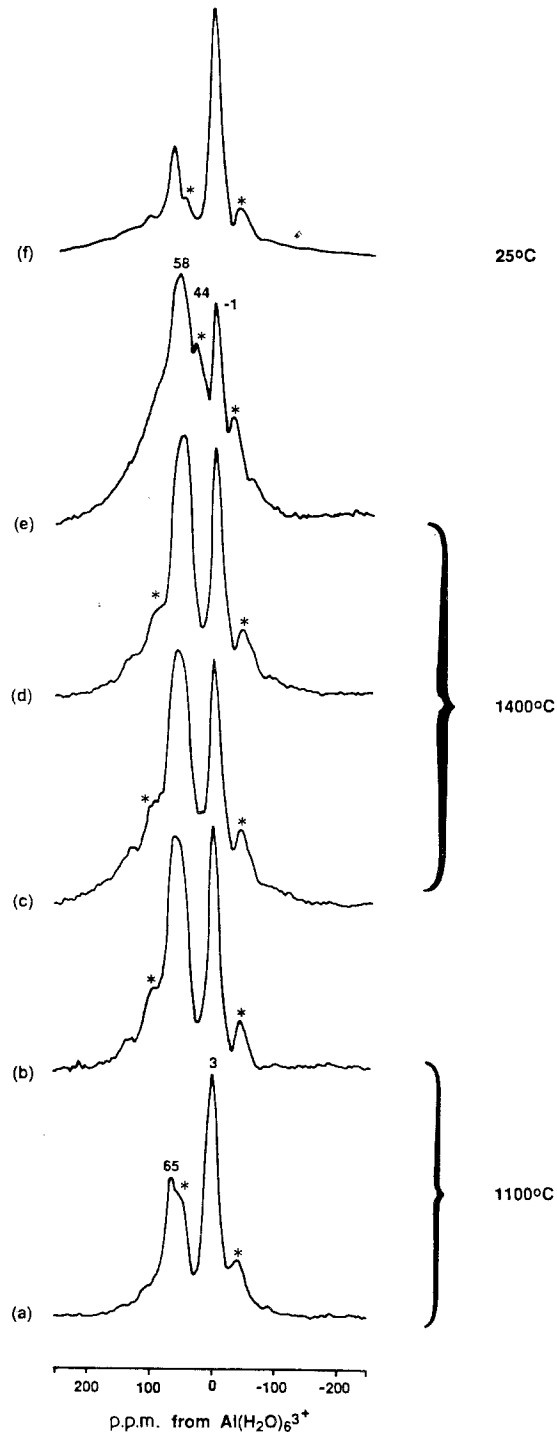

Figure 9 ^{27}Al MAS NMR spectra of (a, c) non-mineralized and (b, d, e) mineralized samples. In order to reveal the presence of mullite resonances which overlap with the spinning sidebands, the latter spectrum was acquired with a slower spinning rate (3.3 kHz) than that used (~ 4.5 kHz) for the other spectra. The spectrum of a standard γ-alumina is shown for comparison in (f). (*) Spinning sidebands.

4.4. Action on amorphous silica and on cristobalite

Above 1100 °C, ^{7}Li T_1 values continue to change; however, the ^{27}Al MAS NMR spectra of MS and NMS do not vary significantly. The lineshape of the mullite ^{29}Si resonance at − 87 p.p.m. does not change either. One would not expect, therefore, ^{7}Li to be associated with either the aluminium or silicon matrices of mullite but with the amorphous silica and/or cristobalite phases. Indeed, in MS above ~ 1100 °C

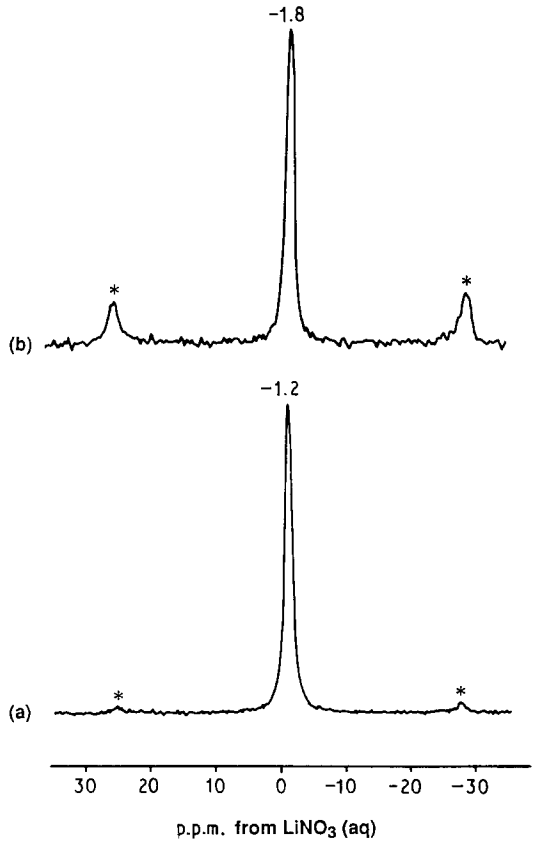

Figure 10 ^{7}Li MAS NMR spectra of mineralized kaolinite (a) at room temperature and (b) calcined in air for 1 h at 600 °C. (*) Spinning sidebands.

the amorphous silica crystallizes as cristobalite. It is known [20] that SiO_2 glass crystallizes more rapidly in the presence of oxide impurities, and that the onset of crystallization occurs at lower temperatures. This is in accord with our observation that cristobalite crystallizes first in MS than in NMS. Pure SiO_2 glass contains almost exclusively strong ≡Si–O–Si≡ bonds. Diffusional insertion of cations such as Li^+ breaks these bonds according to the scheme [21]

$$\equiv Si\text{–}O\text{–}Si\equiv \; + \; Li_2O \; \rightarrow \; \equiv Si\text{–}O\text{–}Li|Li\text{–}O\text{–}Si\equiv \qquad (1)$$

Weaker Si–O–Li bonds facilitate the transition of the glass structure to a crystalline framework.

At 1300–1400 °C, cristobalite vitrifies in MS. Brown *et al.* [22] reported that at 1450–1500 °C, non-mineralized kaolinite samples undergo a similar transformation but we did not observe it even at temperatures as high as 1500 °C. Inspection of the phase diagram for the system SiO_2–Al_2O_3 (see also West [19]) reveals that kaolinite begins to melt above 1595 °C but is not completely liquid until well above 1800 °C. On the other hand, montmorillonite clays such as bentonite, melt at ~ 1300 °C. This is due not only to much higher silica-to-alumina ratios (~ 4:1) but also to the presence of alkali cations. Vitrification observed in MS treated at between 1300 and 1400 °C and then quenched is probably caused by the lowering of the melting point of cristobalite by the mineralizer. The glass is then produced by the rapid cooling of molten cristobalite. Our work was not carried out under equilibrium conditions and thus the results are not directly comparable with the published phase diagrams. All the same, the phase diagram for SiO_2–LiO_2 system [23] shows that the liquid temperature should drop significantly for a concentration of lithium similar to that used here, although not by as much as we observed. Furthermore, the viscosity of a binary liquid silicate system at 1400 °C, 5 mol % Li_2O:SiO_2 has been reported [24] to be two orders of magnitude lower than that of pure SiO_2, and the energy of activation of viscous flow of SiO_2 decreases significantly, which indicates that the structure of the melt has changed.

4.5. Lithium aluminosilicates (LAS)

Neither the XRD patterns nor the FTIR spectra provide any evidence for the presence of either crystalline or amorphous LAS in MS. Nevertheless, it has been reported [17] that when kaolinite samples are heated with a large excess of certain salts (17:1 by weight), both crystalline and amorphous LAS are

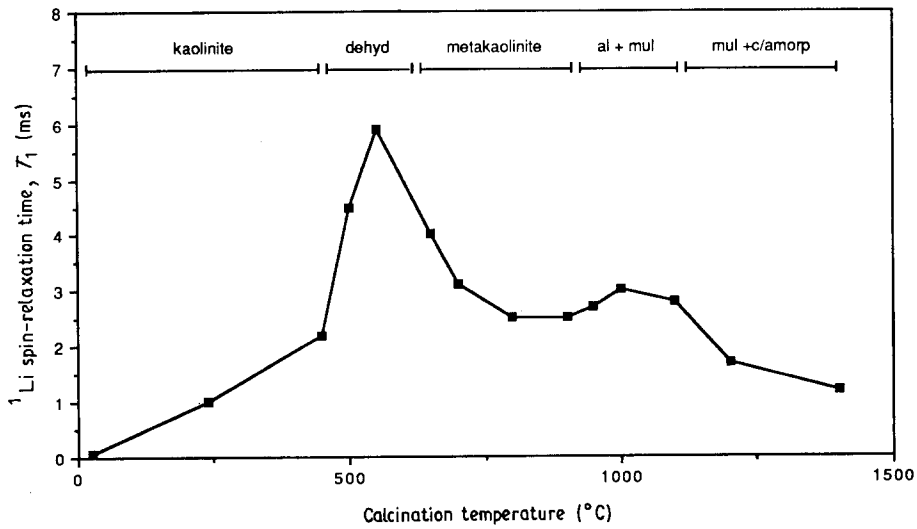

Figure 11 Variation of the ^{7}Li spin-lattice relaxation time (T_1) as a function of the temperature of calcination. For the room temperature sample $T_1 = 45 \pm 4$ ms; for the other samples T_1 ranges from 1.2–5.8 ± 0.2 s. Note that the T_1 values change significantly when some important structural event occurs. "Dehyd", dehydration; "al + mul", γ-alumina type spinel and mullite; "mul + c/amorph", mullite and cristobalite/amorphous silica.

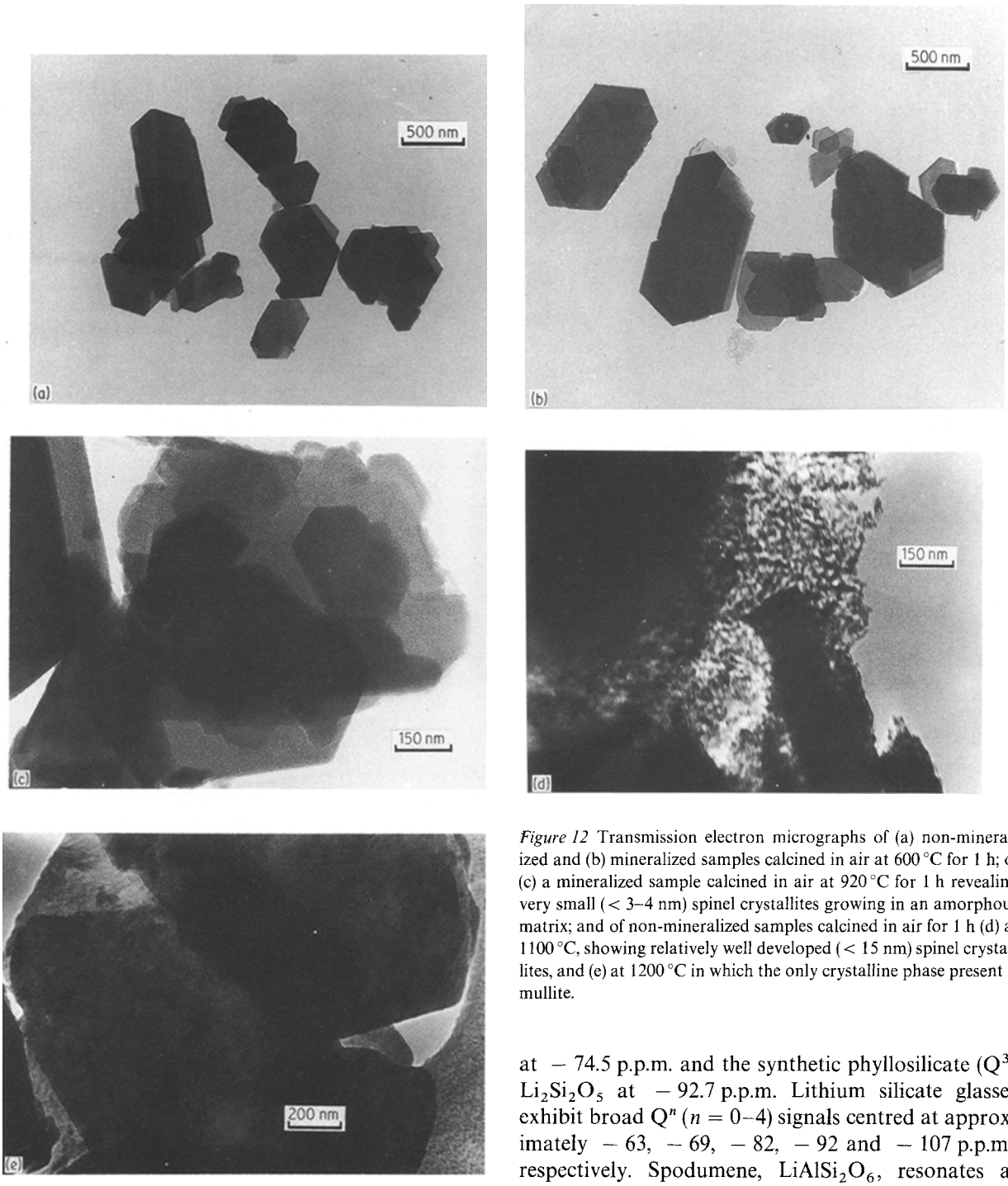

Figure 12 Transmission electron micrographs of (a) non-mineralized and (b) mineralized samples calcined in air at 600 °C for 1 h; of (c) a mineralized sample calcined in air at 920 °C for 1 h revealing very small (< 3–4 nm) spinel crystallites growing in an amorphous matrix; and of non-mineralized samples calcined in air for 1 h (d) at 1100 °C, showing relatively well developed (< 15 nm) spinel crystallites, and (e) at 1200 °C in which the only crystalline phase present is mullite.

produced. Others investigated the formation of LAS by reacting kaolinite or metakaolinite with lithium salts [16, 25] but the presence of LAS was never reported in studies similar to ours [3, 15]. Our ^{29}Si MAS NMR results indicate that no significant amounts of LAS are formed. The lineshapes of the ^{29}Si resonances in the spectra of MS and NMS are very similar, and the only difference is the temperature at which phase transformations occur. If significant amounts of LAS were formed, distinct lineshapes and new ^{29}Si signals would be seen in the spectra of MS. We stress that NMR does not preclude the presence of small amounts of LAS. According to Engelhardt and Michel ([11] and references therein), synthetic sorosilicates (Q^1) such as $Li_6Si_2O_7$ give a resonance at -72.4 p.p.m.; the synthetic single chain (Q^2) Li_2SiO_3 at -74.5 p.p.m. and the synthetic phyllosilicate (Q^3) $Li_2Si_2O_5$ at -92.7 p.p.m. Lithium silicate glasses exhibit broad Q^n ($n = 0$–4) signals centred at approximately -63, -69, -82, -92 and -107 p.p.m., respectively. Spodumene, $LiAlSi_2O_6$, resonates at -91.6 and $Q^n(m\text{Al})$ lithium glasses of different compositions at -90.5, -79.9 and -75.0 p.p.m. for $m = 0$, 1 and 2, respectively.

5. Conclusions

Addition of lithium nitrate to kaolinite before calcination causes:

1. diffusion of Li^+ ions into the bulk of the crystals and stabilization of the kaolinite structure by an additional 15–20 °C;
2. inhibition of the formation of five-fold Al in metakaolinite;
3. crystallization of γ-alumina type spinel from metakaolinite at a lower temperature (~ 920 °C) with a simultaneous retardation of the transformation of the silicon matrix which remains more disordered than in non-doped samples;

4. crystallization of spinel phase (1100 °C) and amorphous silica (1200 °C) in mullite and cristobalite at lower temperatures; earlier vitrification of cristobalite (just above 1300 °C).

No evidence was found for the presence of lithium aluminosilicates. Nevertheless, the possibility that small amounts of these are present cannot be excluded.

Acknowledgements

J. R. and J. K. are grateful to ECC International Limited for support and for providing kaolinite samples, and to the University of Aveiro for support.

References

1. C. W. PARMELEE and A. R. RODRIGUEZ, *J. Am. Ceram. Soc.* **25** (1942) 1.
2. S. P. CHAUDHURI, *Trans. Brit. Ceram. Soc.* **28** (1969) 24.
3. J. LEMAITRE and B. DELMON, *J. Mater. Sci.* **12** (1977) 2056.
4. D. N. HINCKLEY, in "Clays and Clay Minerals, Proceedings of the 13th National Conference", Madison, Wisconsin, 1964, edited by W. F. Bradley and S. W. Bailey (Pergamon Press, New York, 1963) pp. 220–35.
5. K. SRIKRISHNA, G. THOMAS, R. MARTINEZ, M. P. CORRAL, S. AZA and J. S. MOYA, *J. Mater. Sci.* **25** (1990) 607.
6. J. ROCHA and J. KLINOWSKI, *Phys. Chem. Min.* **17** (1990) 179.
7. H. J. PERCIVAL, J. F. DUNCAN and P. K. FOSTER, *J. Amer. Ceram. Soc.* **57** (1974) 57.
8. J. ROCHA and J. KLINOWSKI, *Angew. Chim.* **29** (1990) 553.
9. J. F. LAMBERT, W. S. MILLMAN and J. J. FRIPIAT, *J. Amer. Chem. Soc.* **111** (1989) 3517.
10. J. SANZ, A. MADANI, J. M. SERRATOSA and S. AZA, *J. Amer. Ceram. Soc.* **71** (1988) C-418.
11. G. ENGELHARDT and D. MICHEL, "High-resolution solid-state NMR of silicates and zeolites" (Wiley, New York, 1987).
12. E. GÖBEL, W. MÜLLER-WARMUTH and H. OLYSCHLÄGER, *J. Magn. Reson.* **36** (1979) 371.
13. M. BULENS and B. DELMON, *Bull. Soc. Chim. Belg.* **86** (1977) 405.
14. M. BULENS, A. LEONARD and B. DELMON, *J. Amer. Ceram. Soc.* **61** (1978) 81.
15. C. S. F. GOMES, *Miner. Petrogr. Acta* **29A** (1985) 381.
16. A. G. VERDUCH and J. S. M. CORRAL, in "Proceedings of the International Clay Conference", Madrid (1972) p. 131.
17. L. HELLER-KALLAI, *Clay Min.* **13** (1978) 221.
18. S. A. T. REDFERN, *ibid.* **22** (1987) 447.
19. A. R. WEST, "Solid-state chemistry and its applications" (Wiley, Chichester, 1984).
20. R. B. SOSMAN, "The phases of silica" (Rutgers University Press, New Brunswick, 1965).
21. G. H. FRISCHAT, "Ionic diffusion in oxide glasses: Diffusion and defect monographs series", 3/4 (Trans Tech, Aedermannsdorf, Switzerland, 1975).
22. I. W. M. BROWN, K. J. D. MACKENZIE, M. E. BOWDEN and R. H. MEINHOLD, *J. Am. Ceram. Soc.* **68** (1985) 298.
23. ACS, "Phase diagrams for ceramists", compiled at the National Bureau of Standards (The American Ceramic Society, Ohio, 1969).
24. A. PAUL, "Chemistry of glasses" (Chapman and Hall, London, New York, 1982).
25. Y. KUBO and Y. YAMABE, "Proceedings of the International Clay Conference", Tokyo, Vol. 1 (1969) p. 915.

Received 15 May
and accepted 26 June 1990